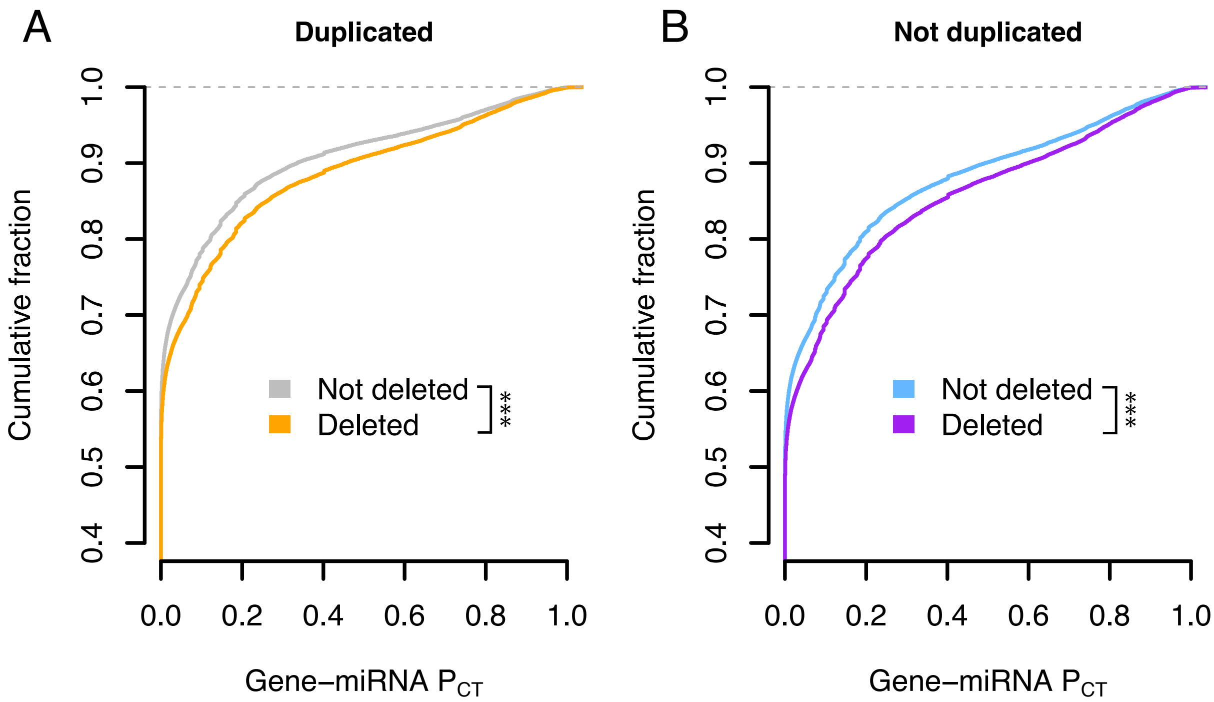

Supplemental Figure S1: Effect of deletion status on autosomal P_{CT} scores. Probabilities of conserved targeting (P_{CT}) of all gene-miRNA interactions involving non-deleted and deleted genes, further stratified as (A) duplicated (grey, n = 69,339 interactions from 4,118 genes; orange, n = 51,514 interactions from 2,916 genes) or (B) not duplicated (purple, n = 72,826 interactions from 3,510 genes; blue, n = 80,290 interactions from 3,976 genes). *** $p < 0.001$, two-sided Kolmogorov-Smirnov test.

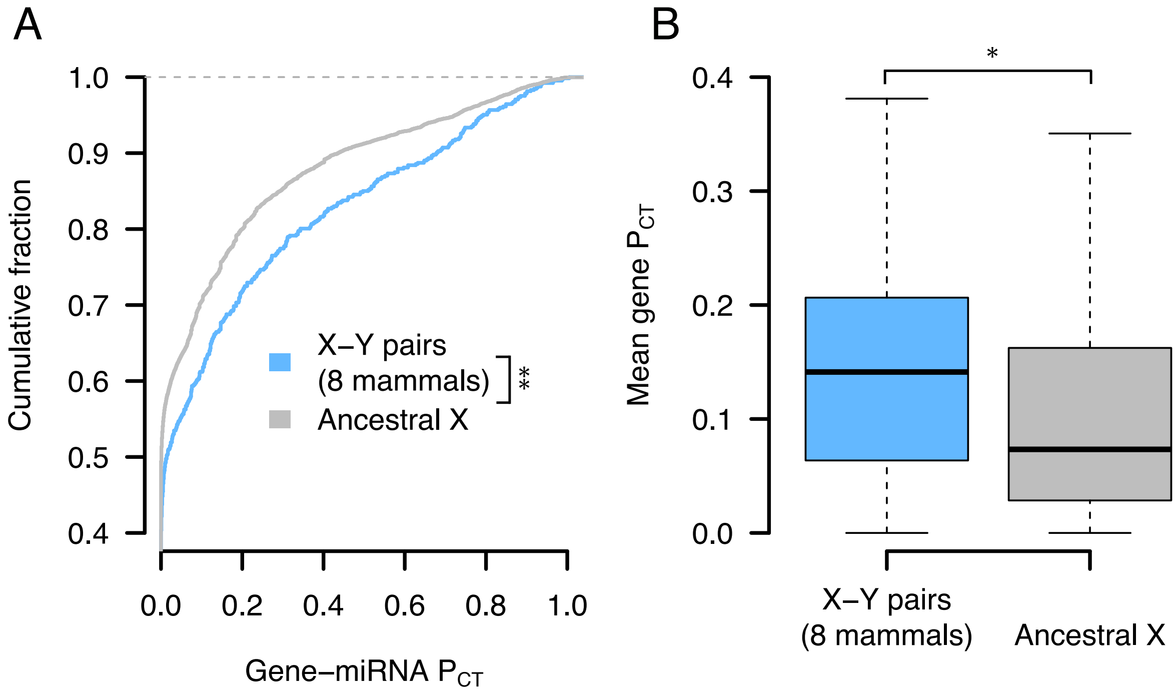

SSupplemental Figure S2: P_{CT} scores of X-Y pairs across 8 mammals. (A) P_{CT} score distributions of all gene-miRNA interactions involving X-Y pairs across eight sequenced mammalian Y chromosomes (n = 647 interactions from 32 genes) and other ancestral X genes (n = 8,831 interactions from 457 genes). ** $p < 0.01$, two-sided Kolmogorov-Smirnov test. (B) Gene-level mean P_{CT} scores. * $p < 0.05$, two-sided Wilcoxon rank-sum test.

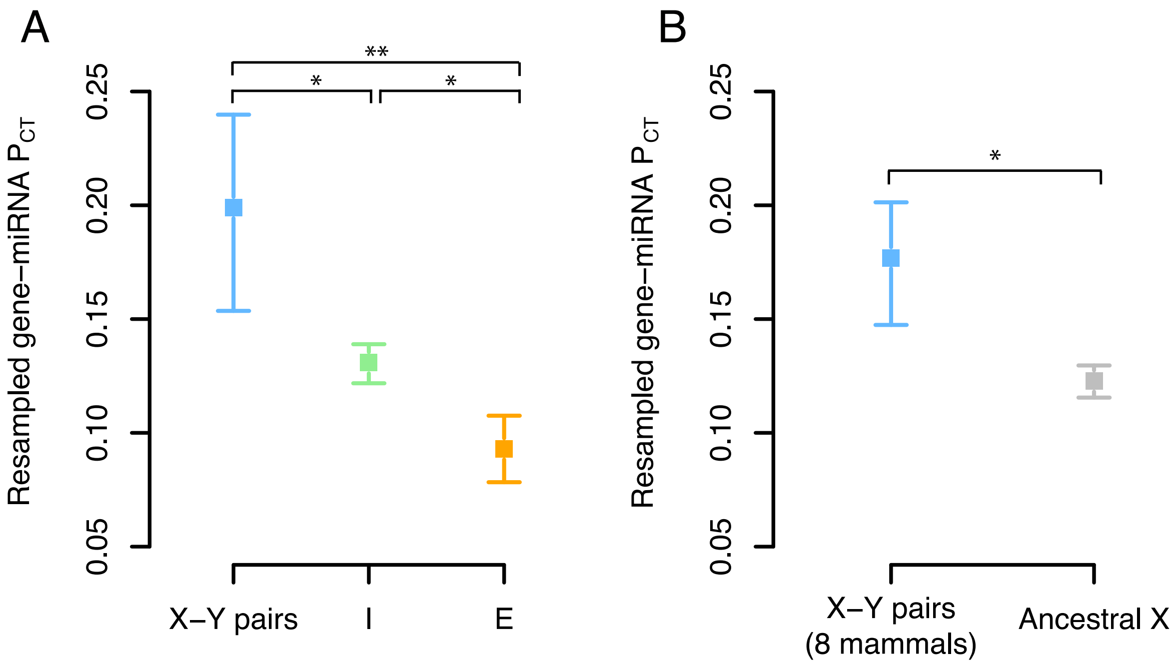

Supplemental Figure S3: Resampled mean P_{CT} scores of X-linked genes. (A) Resampled gene-miRNA P_{CT} scores for human X-Y pairs (n = 15 genes), X-inactivated genes (n = 329 genes) and X escape genes (n = 56 genes). (B) Resampled gene-miRNA P_{CT} scores for X-Y pairs across eight mammals (n = 32 genes) and genes with no Y homolog in any of eight mammals (n = 457 genes). Points and error bars represent the median and 95% confidence intervals from 1,000 gene samplings with replacement. * $p < 0.05$, ** $p < 0.01$, empirical p-value computed as the fraction of random non-overlapping gene sets with a median difference in P_{CT} score at least as large as the true difference.

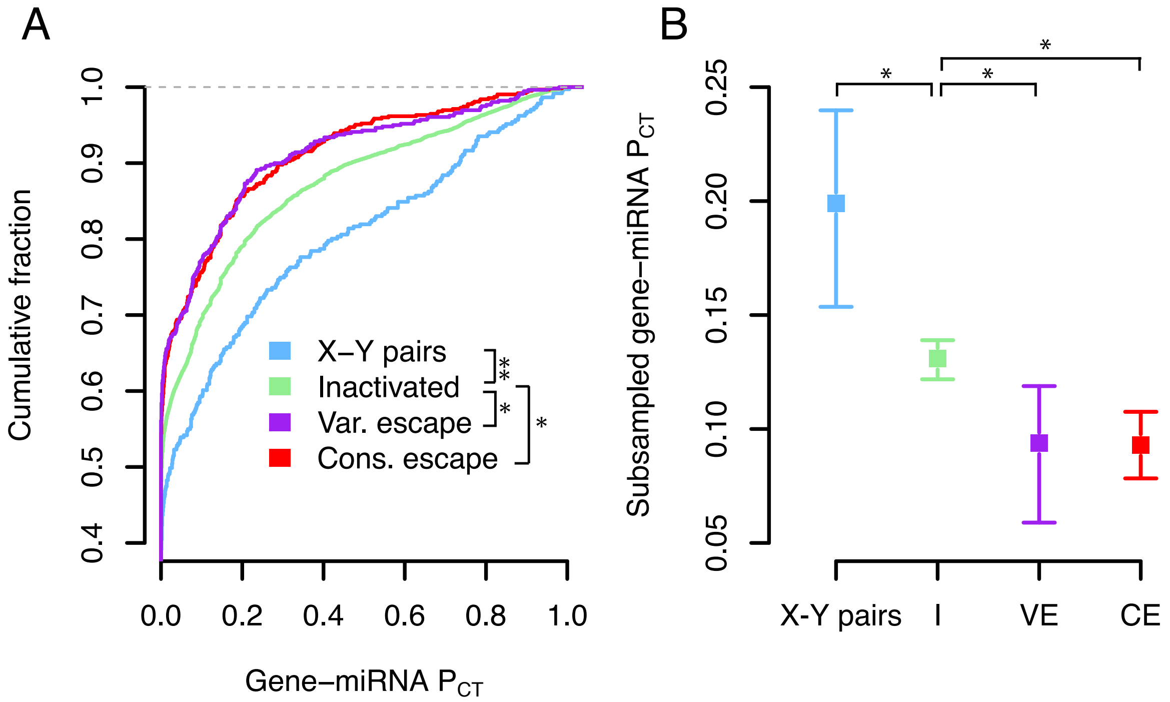

Supplemental Figure S4: P_{CT} score comparisons with consistent and variable escape genes separated. (A) P_{CT} score distributions of all gene-miRNA interactions involving X-Y pairs (n = 371 interactions from 16 genes), X-inactivated genes (n = 6743 interactions from 329 genes), consistent escape genes (n = 567 interactions from 30 genes), or variable escape genes (n = 470 interactions from 26 genes) as defined by Balaton et al (Balaton et al., 2015). * $p < 0.05$, ** $p < 0.01$, two-sided Kolmogorov-Smirnov test. (B) Resampled gene-miRNA P_{CT} scores of gene classes from (A). Points and error bars represent the median and 95% confidence intervals from 1,000 gene samplings with replacement. * $p < 0.05$, empirical p-value computed as the fraction of random non-overlapping gene sets with a median difference in P_{CT} score at least as large as the true difference.

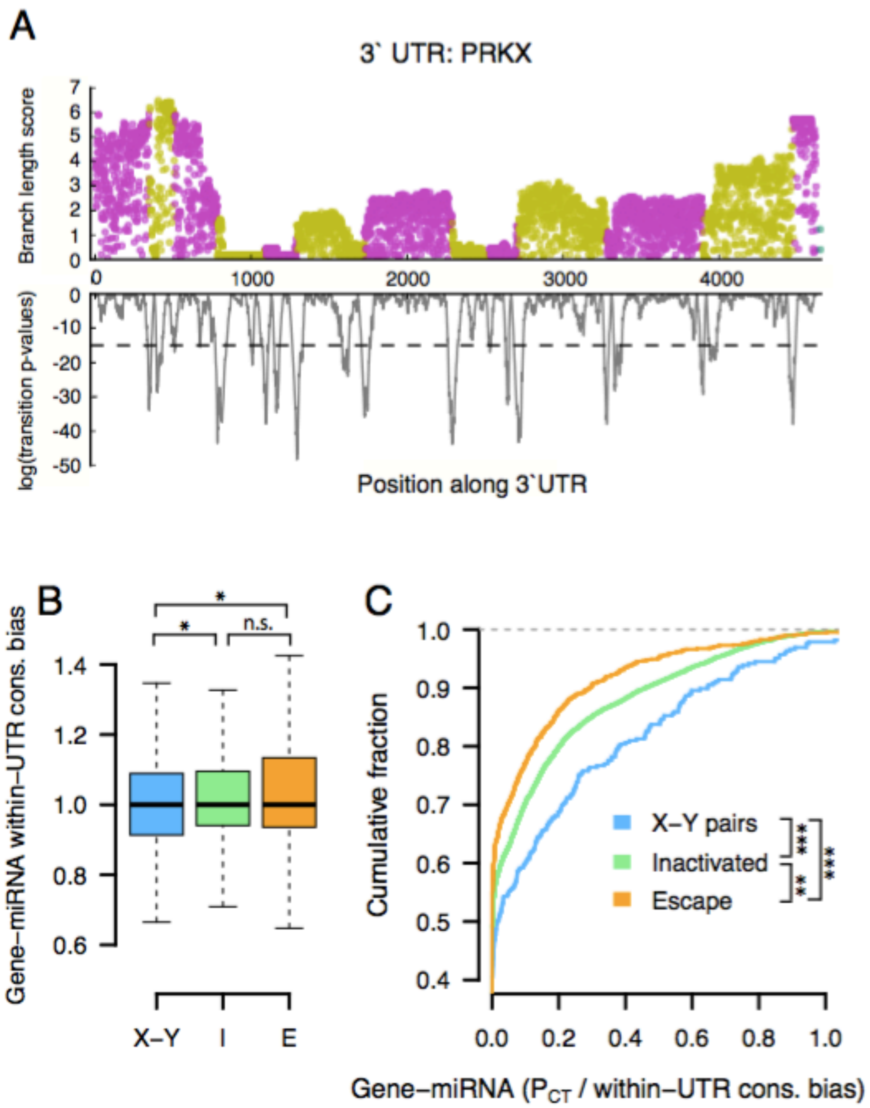

Supplemental Figure S5: Variation in within-UTR conservation does not account for observed differences in P_{CT} score among classes of X-linked genes. (A) Example of step-detection to segment 3` UTRs. Top, base-wise branch length scores; bottom, probabilities of transition to a new section. Dashed line indicates p-value cutoff used to delineate a new section (plotted as alternating magenta/yellow points). (B) Boxplots of within-UTR conservation bias (see Methods) for all gene-miRNA interactions involving classes of X-linked genes. (C) Comparisons of P_{CT} scores normalized by within-UTR bias. **, $p < 0.01$, *** $p < 0.001$, two-sided Kolmogorov-Smirnov test.

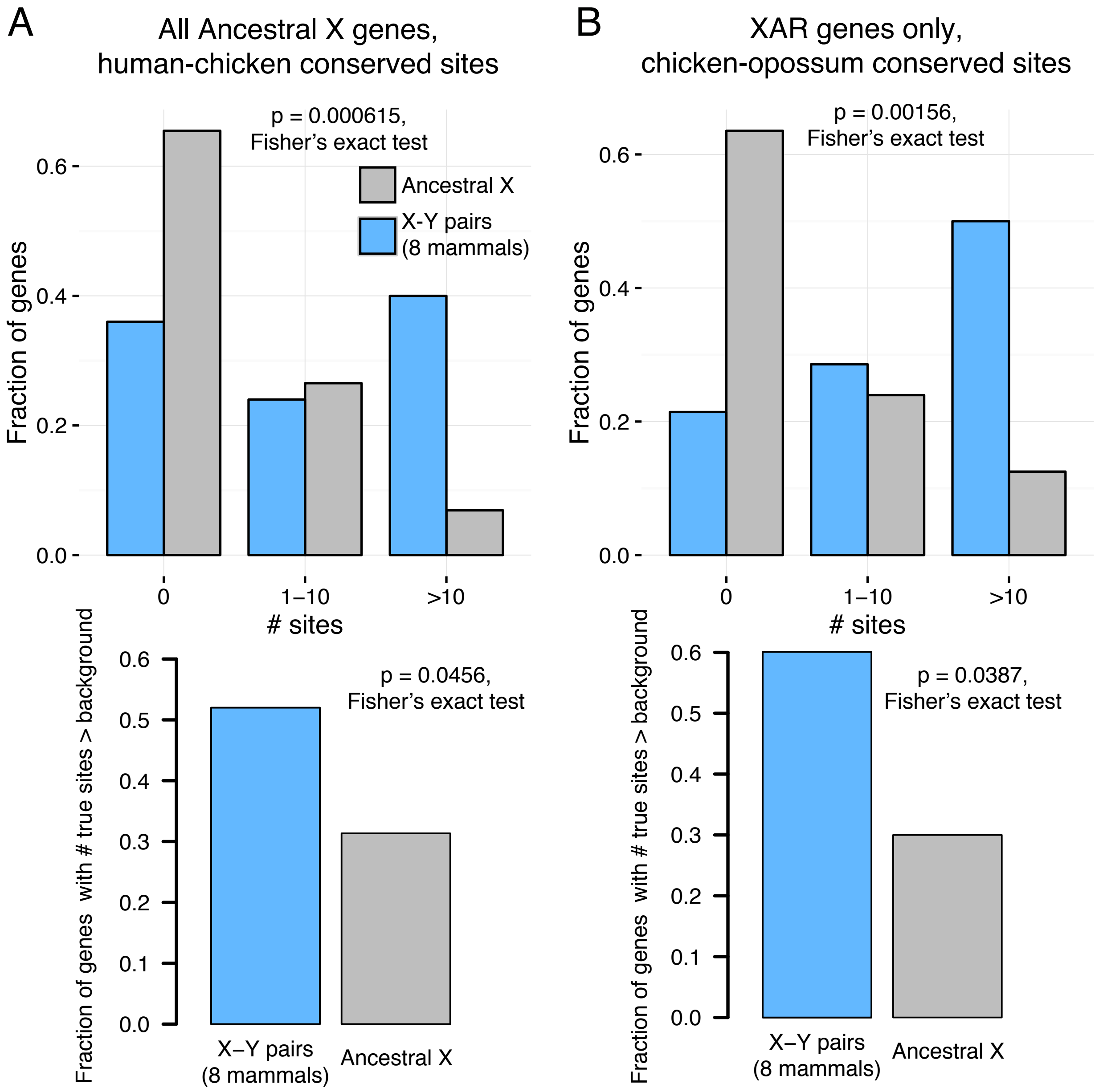

Supplemental Figure S6: Ancestral miRNA targeting of X-Y pairs across 8 mammals. (A) Distributions of sites conserved between 3` UTRs of human and chicken orthologs (top) or comparisons to background expectation (bottom, see Methods) for X-Y pairs across 8 mammals (n = 25) and other ancestral X genes (n = 351). (D) Statistics as in (C), but using sites conserved between chicken and opossum 3` UTRs only for genes in the XAR; X-Y pairs across 8 mammals (n = 15), other ancestral X genes (n = 102).

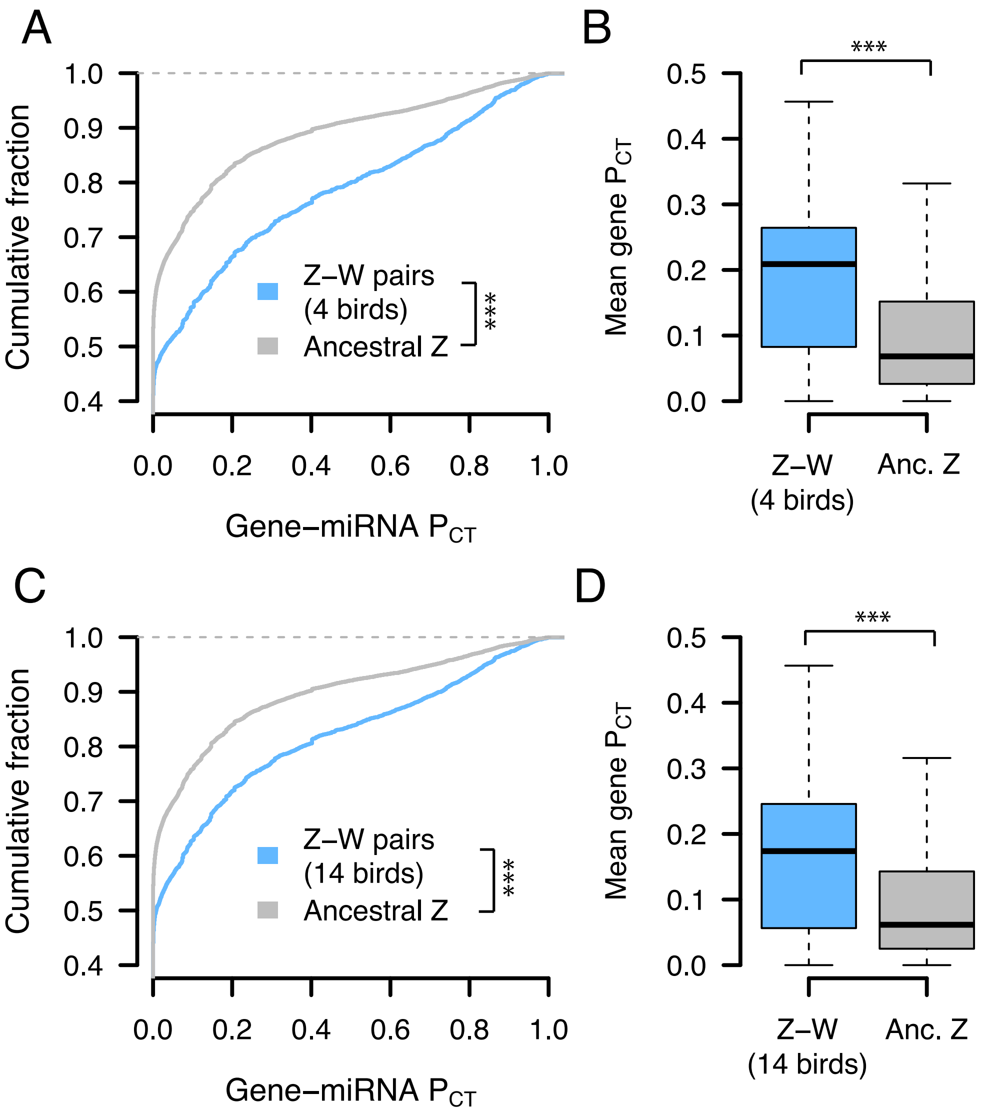

Supplemental Figure S7: P_{CT} scores of Z-W pairs across 4 and 14 birds. (A,C) P_{CT} score distributions of all gene-miRNA interactions (A) Z-W pairs including predictions from three additional birds with male and female genome sequence (n = 2,187 interactions from 78 genes) and other ancestral Z genes (n = 15,357 interactions from 607 genes), or (C) Z-W pairs including read depth-based predictions from 10 additional birds with only female genome sequence (n = 4,458 interactions from 157 genes) and other ancestral Z genes (n = 13,086 interactions from 528 genes) *** $p < 0.001$, two-sided Kolmogorov-Smirnov test. (B,D) Gene-level mean P_{CT} scores. *** $p < 0.01$, two-sided Wilcoxon rank-sum test.

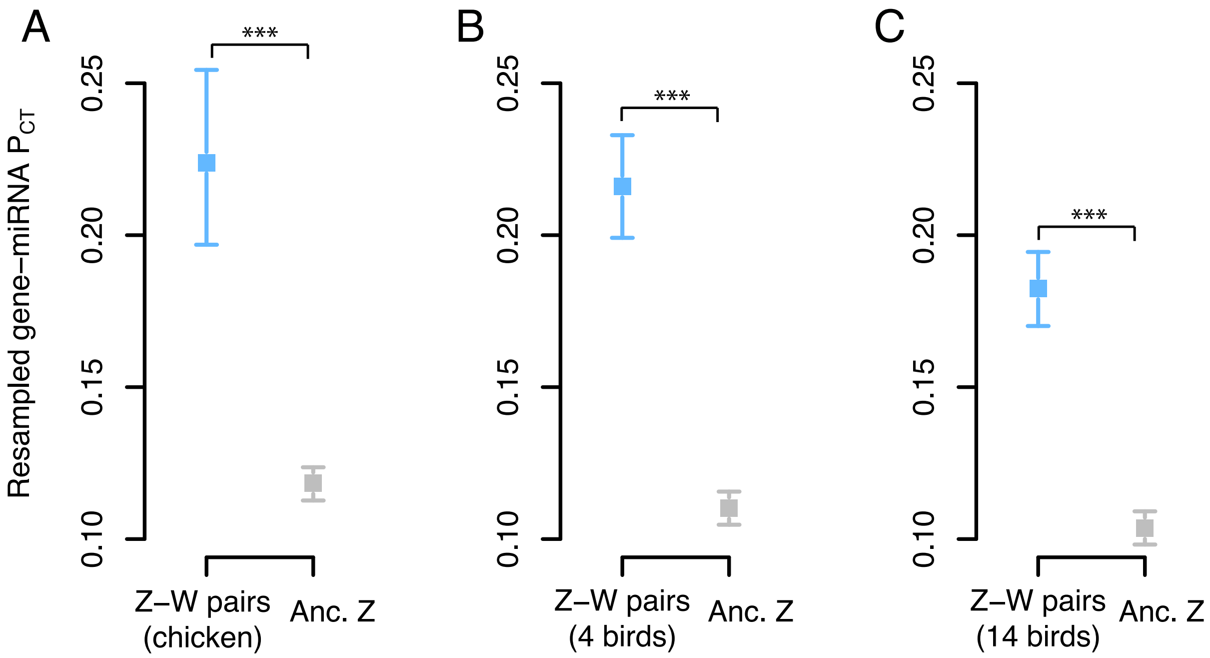

Supplemental Figure S8: Resampled mean P$_{CT}$ scores of Z-linked genes. Gene sets: (A) chicken Z-W pairs (n = 28 genes) and other ancestral Z genes (n = 657 genes), (B) Z-W pairs across four birds (n = 78 genes) compared to the remainder of ancestral Z genes (n = 607 genes), and (C) Z-W pairs across 14 birds (n = 157 genes) compared to the remainder of ancestral Z genes (n = 528 genes). Points and error bars represent the median and 95% confidence intervals from 1,000 gene samplings with replacement. *** $p < 0.001$, empirical p-value computed as the fraction of random non-overlapping gene sets with a median difference in P$_{CT}$ score at least as large as the true difference.

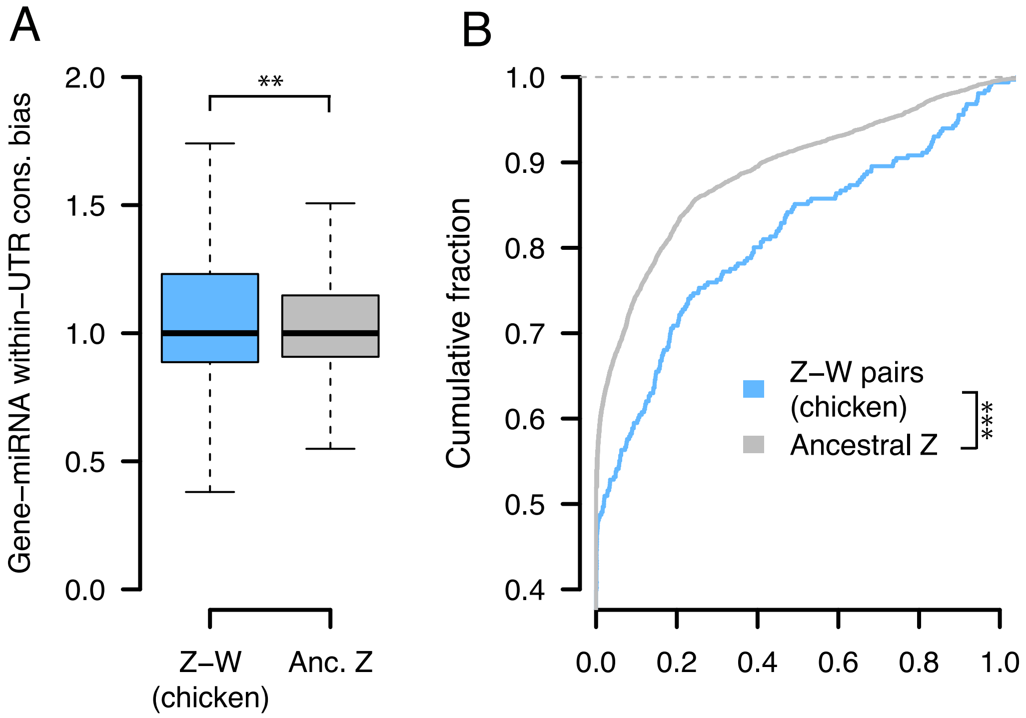

Supplemental Figure S9: Variation in within-UTR conservation cannot account for observed differences in P_{CT} score among classes of Z-linked genes. (A) Boxplots of within-UTR conservation bias (see Methods) for all gene-miRNA interactions involving chicken Z-W pairs or other ancestral X genes. Numbers of interactions and genes as in Figure 4A. ** $p < 0.01$, two-side Wilcoxon rank-sum test. (B) Comparisons of P_{CT} scores normalized by within-UTR bias. *** $p < 0.001$, two-sided Kolmogorov-Smirnov test.

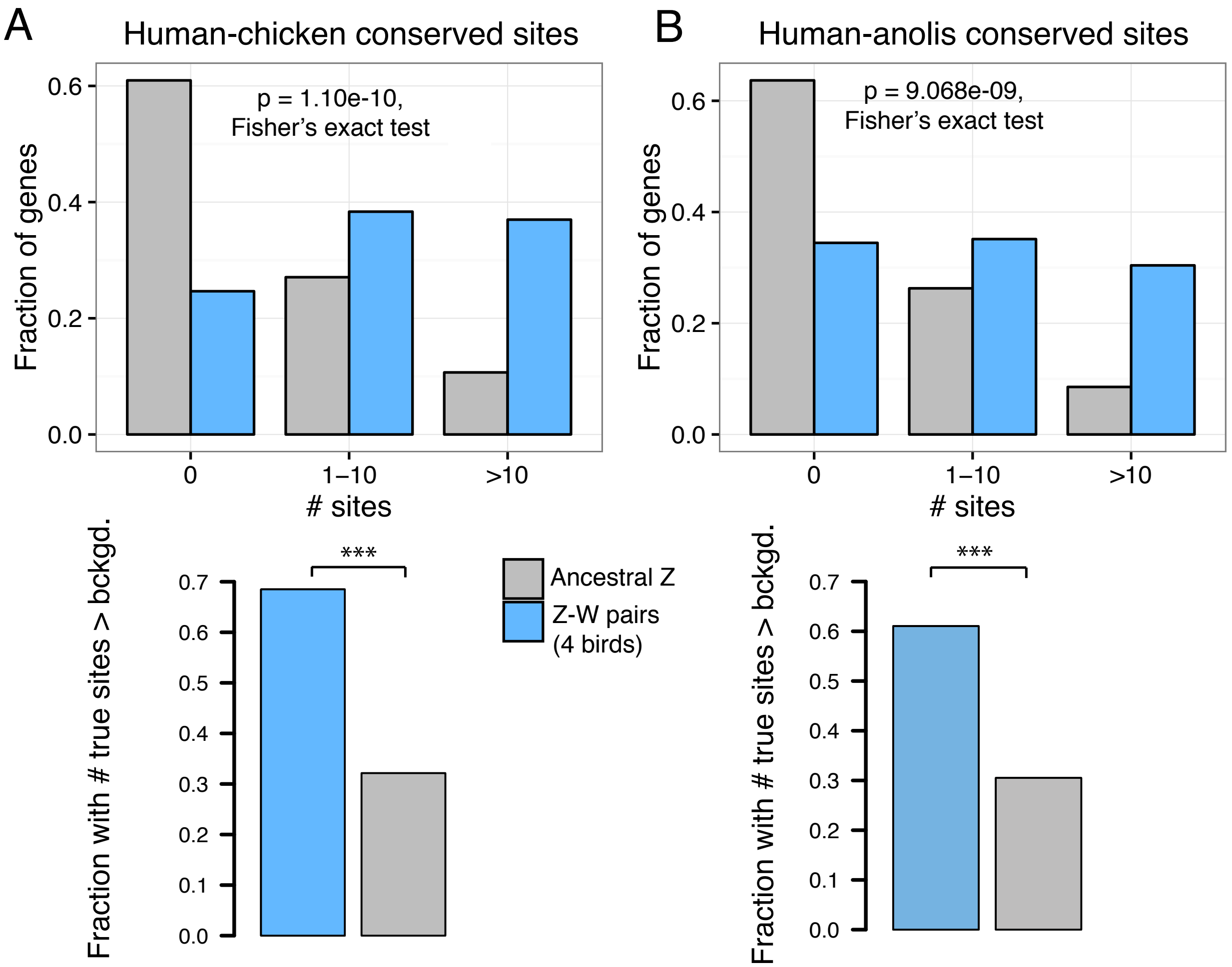

Supplemental Figure S10: Ancestral miRNA targeting of Z-W pairs across 4 birds. (A) Distributions of sites conserved between 3` UTRs of human and chicken orthologs (top) or comparisons to background expectation (bottom, see Methods) for Z-W pairs across chicken and three additional birds with male and female genome sequence (4 birds, n = 73) and other ancestral Z genes (n = 532). (D) Statistics as in (C), but using sites conserved between human and anolis 3` UTRs; Z-W pairs across 4 birds (n = 73), other ancestral Z genes (n = 527). *** p < 0.001, two-sided Fisher's exact test.

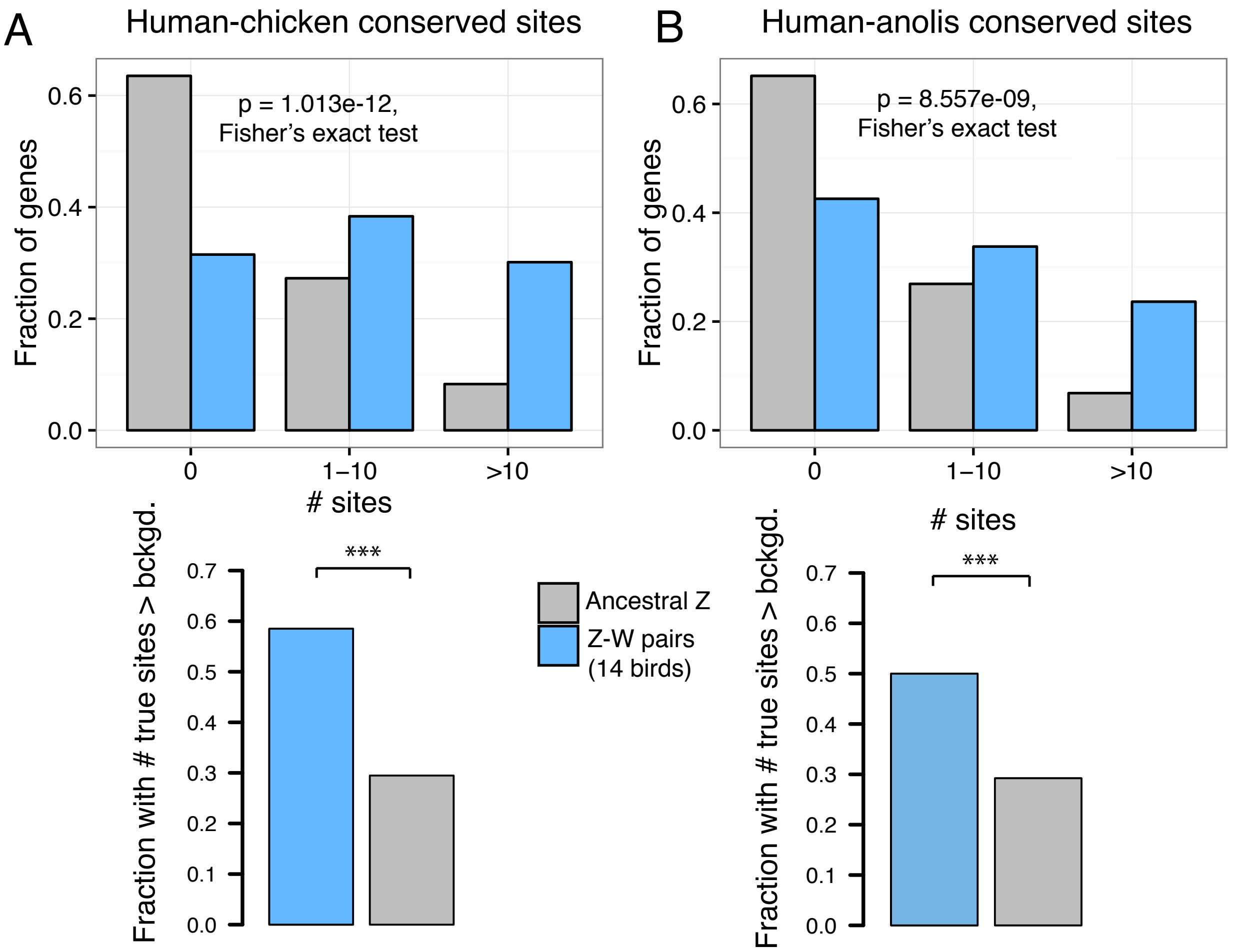

Supplemental Figure S11: Ancestral miRNA targeting of predicted Z-W pairs across 14 birds. (A) Distributions of sites conserved between 3` UTRs of human and chicken orthologs (top) or comparisons to background expectation (bottom, see Methods) for Z-W pairs in chicken, predicted in three additional birds with male and female genome sequence, and predicted based on read depth from 10 additional birds with only female genome sequence (14 birds, n = 147) and other ancestral Z genes (n = 458). (D) Statistics as in (C), but using sites conserved between human and anolis 3` UTRs; Z-W pairs across 14 birds (n = 147), other ancestral Z genes (n = 453)

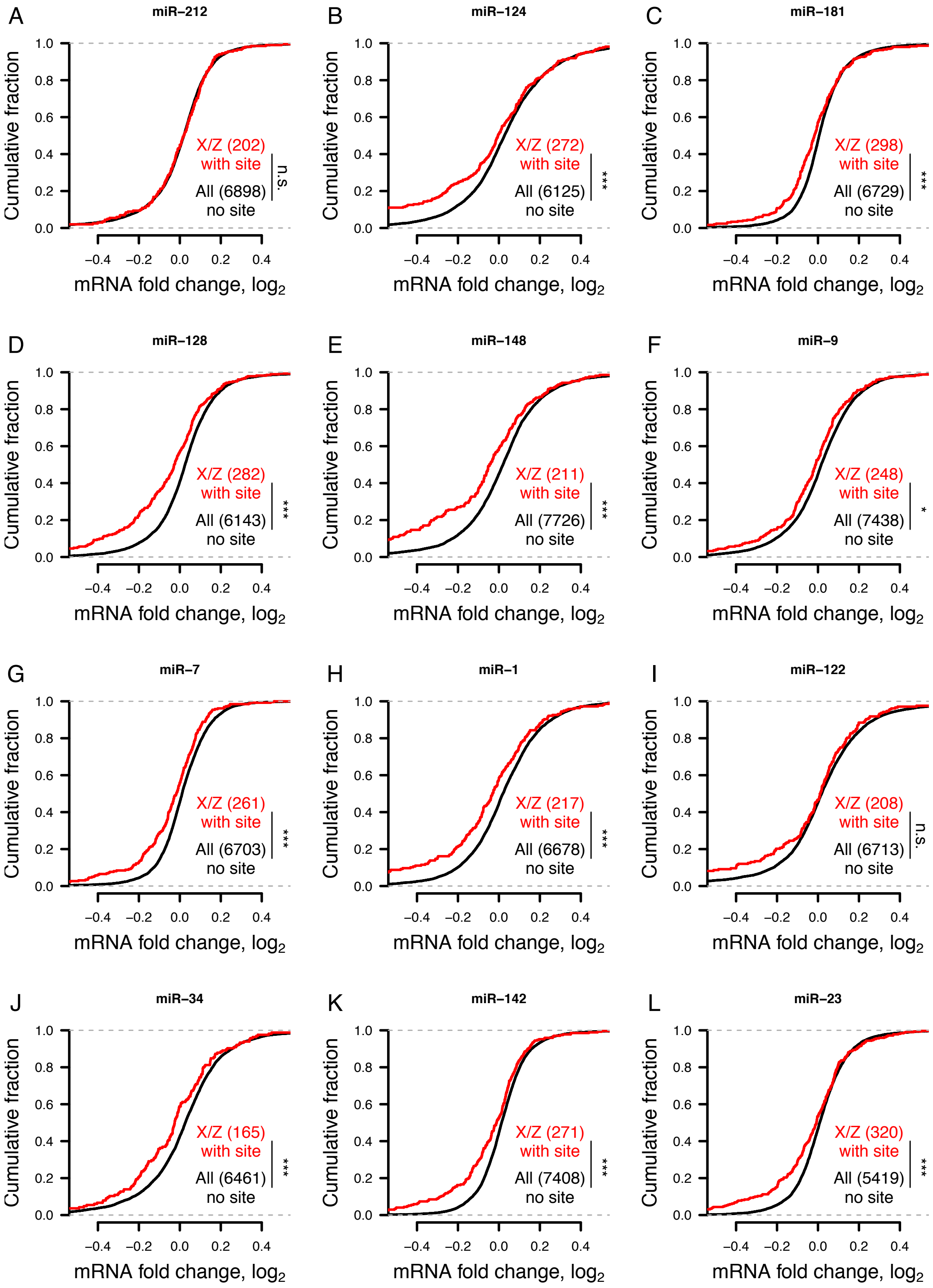

Supplemental Figure S12: Gene expression changes following small RNA transfections in human HeLa cells. * $p < 0.05$, *** $p < 0.001$, two-sided K-S test.

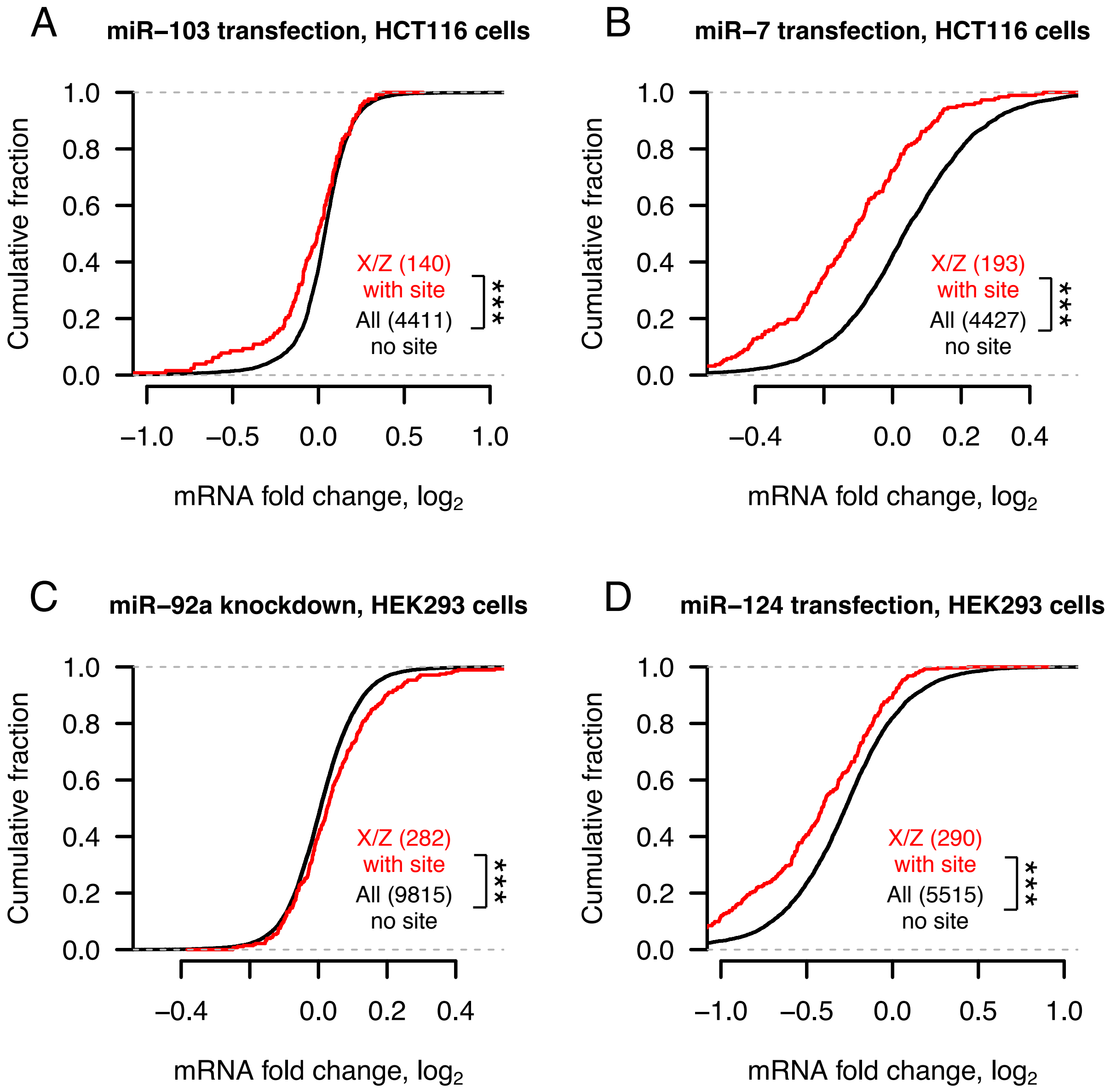

Supplemental Figure S13: Gene expression changes following transfection or knockdown of additional miRNAs in human HCT116 or HEK293 cells. *** $p < 0.001$, two-sided Kolmogorov-Smirnov test.

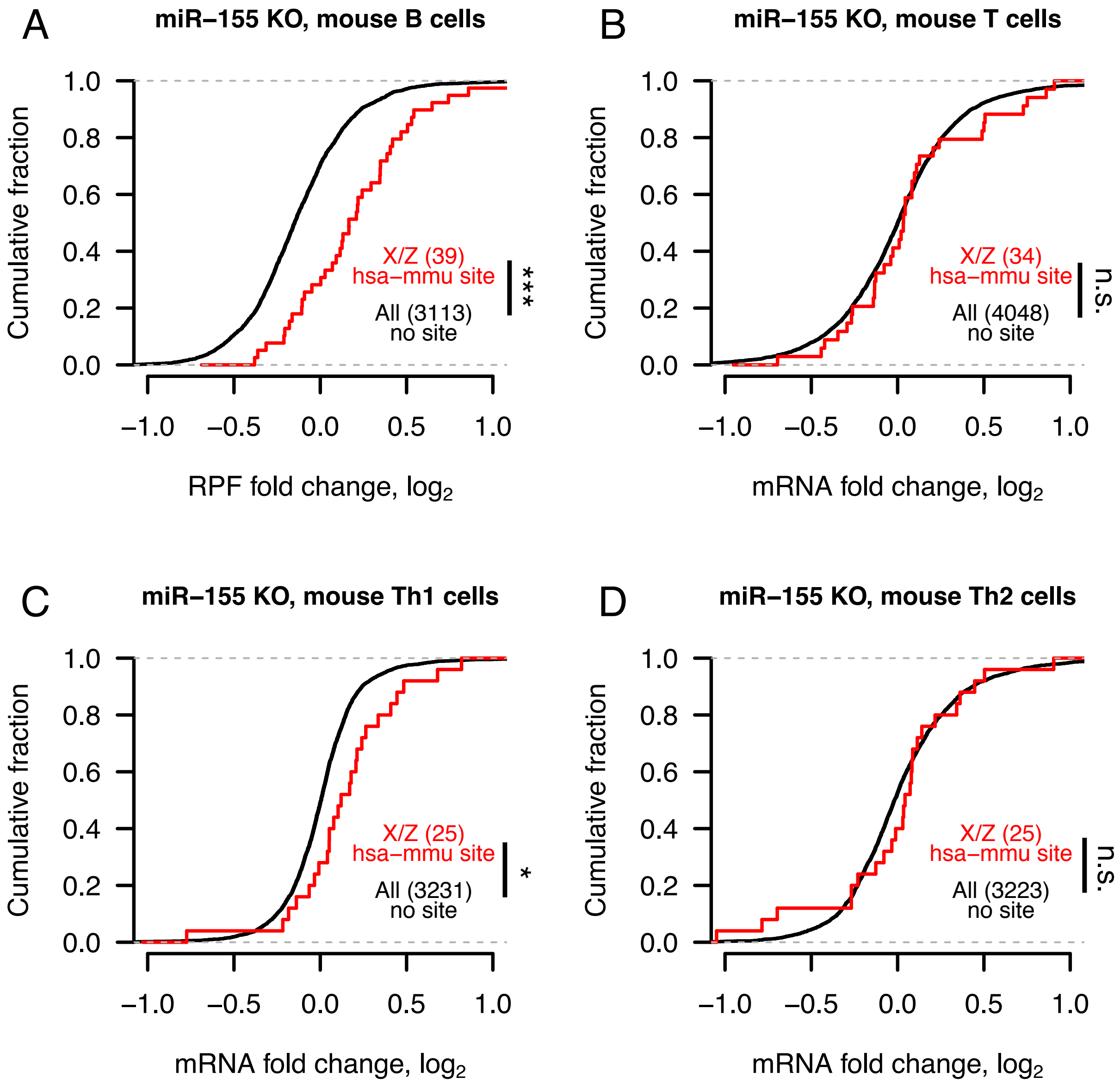

Supplemental Figure S14: Changes in mRNA stability and translational efficiency and gene expression following miR-155 knockout in mouse immune cells. In each case, mouse orthologs of X- or Z-linked genes containing a human-mouse-conserved (hsa-mmu) miR-155 site were compared to mouse genes containing only nonconserved miR-155 sites. * $p < 0.05$, *** $p < 0.001$, two-sided Kolmogorov-Smirnov test.

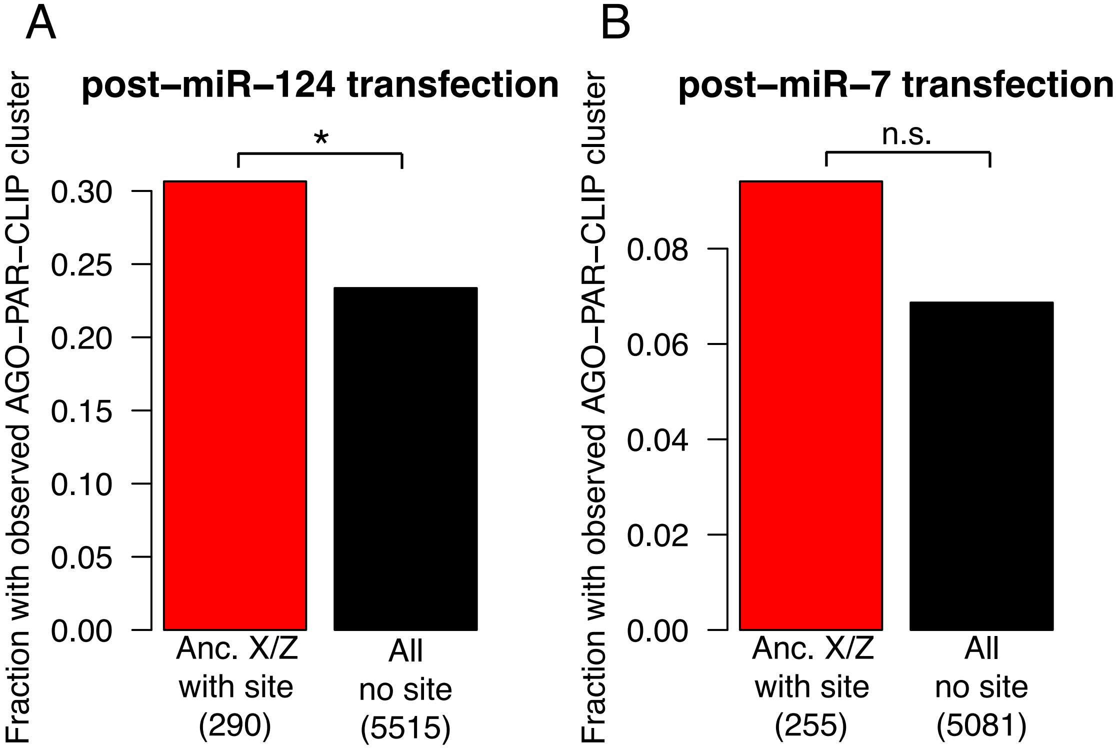

Supplemental Figure S15: Argonaute binding measured by high-throughput crosslinking-immunoprecipitation (CLIP) following miRNA transfection in HEK293 cells. * $p < 0.05$, two-sided Fisher's exact test.